Numerical Calculation of the Stability of Parallel Flows

James H. Stuhmiller*
JAYCOR, Del Mar, Calif.

A numerical approach to solve for perturbations to the two-dimensional, incompressible Navier-Stokes equations is presented and is used to study the stability and evolution of disturbances in a parallel-flow boundary layer. Previous numerical approaches have used stream function and/or vorticity formulations that take advantage of the special properties of two-dimensional flow. The present method solves a finite-difference form of the momentum equations and therefore may be extended to three dimensions more readily. Computations using this technique are compared with the result of linear stability theory for small-amplitude disturbances and are found to give satisfactory agreement, whereas calculations at large amplitude support the conjecture that nonlinear effects can be destabilizing.

Nomenclature

i	= index denoting cell columns
I	= index of rightmost column
j	= index denoting cell rows
J	= index of topmost row
n	= index denoting time level
p,P	= fluid pressure divided by mass density
R	= Reynolds number ($U_\infty \delta/\nu$)
T	= period of oscillation of disturbance
u,U	= streamwise component of fluid velocity
U_∞	= freestream velocity
x	= streamwise coordinate
y	= normal coordinate
α	= dimensionless wave number ($2\pi\delta/\lambda$)
β	= dimensionless frequency of oscillation ($2\pi\delta/U_\infty T$)
δ	= displacement thickness of boundary layer ($1.72\sqrt{\nu x/U_\infty}$)
$\delta x,\delta y,\delta t$	= finite space and time increments
∇^2	= Laplacian operator ($\partial^2/\partial x^2 + \partial^2/\partial y^2$)
θ	= logarithm energy change
λ	= wavelength of disturbance
ν	= kinematic viscosity of fluid

I. Introduction

ONE of the principal interactions between a fluid and a solid structure is the tangential force due to relative motion. At low velocities, when the flow is still laminar, the drag force is small, but at higher speeds, when the flow has become turbulent, the drag, as well as the heat transfer, increases enormously. It is of practical interest to be able to understand the mechanisms leading to the transition from laminar to turbulent flow and to be able to predict and control that phenomenon.

The onset of turbulence is preceded by a motion in the boundary layer which is certainly three-dimensional and probably highly nonlinear. Any theory that would explain the transition process must address these two issues in some manner. At its initial stages, however, transition appears to involve fairly regular, small-amplitude, two-dimensional disturbances that are capable of extracting energy from the mean flow and thereby grow rapidly. This motion is within the power of analysis to investigate as an eigenvalue problem, and, consequently, it has been studied extensively.

Received Dec. 14, 1977; revision received May 8, 1978.

Index categories: Boundary-Layer Stability and Transition; Computational Methods.

*Senior Scientist, Mathematical Modeling Group. Member AIAA.

The extension of these results to true initial-value problems, large amplitudes, and three dimensions has proved to be quite difficult for analysis, and so it is desirable to develop other approaches to assist in understanding these effects. One promising approach is the direct, numerical solution of the governing equations. Encouraging results already have been obtained by Fasel[1] and Murdock[2] using equations of motion cast in stream-function and/or vorticity forms. Fasel employed a three-time-level finite-difference solution algorithm, whereas Murdock has combined an orthogonal function expansion in the spatial directions with a finite-difference representation in time. Both approaches were directed at temporally periodic, spatially growing disturbances. The two methods appear to give good agreement with linear analysis and with one another.

The present work explores another numerical approach: the finite-difference solution of the momentum form of the Navier-Stokes equations. Three variables (two velocities and a pressure) must now be calculated instead of two (a stream function and vorticity), however, the numerical technique is extended readily to three dimensions, where the concept of a stream function no longer is valid. The finite-difference algorithm used differs from that of Fasel in two respects. The present scheme introduces no numerical viscosity into the solution, whereas Fasel's scheme is slightly dissipative. Second, the present scheme requires storing the flow information at only one time level instead of at two levels, as in Fasel's approach. The consideration of computer storage may be a critical one when three-dimensional calculations are attempted. Both schemes involve systems of nonlinear algebraic equations which must be solved iteratively. A final, important distinction is that spatially periodic, temporally growing disturbances are considered in the present work. This requires a formulation of the problem boundary conditions different from those of Fasel and Murdock. However, on or near the neutral curve, where all of the validating comparisons are made, the two solutions are identical.

The work presented here describes the details of the problem formulation and numerical solution procedure as applied to spatially periodic, parallel flows. Comparisons with the results of linear analysis are made and verify the correctness of the numerical solutions. Finally, the effects of large amplitude on subcritical stability are investigated and indicate that nonlinear effects can be destabilizing.

II. Mathematical Formulation

The motion of the fluid is assumed to be described by the two-dimensional, incompressible, time-dependent Navier-Stokes equations. Normalizing the spatial distances by the displacement thickness of the boundary layer δ, the velocities

by the freestream value U_∞, and time by δ/U_∞, the equations of motion become

$$\frac{\partial u}{\partial t}+u\frac{\partial u}{\partial x}+v\frac{\partial u}{\partial y}+\frac{\partial p}{\partial x}=\frac{1}{R}\nabla^2 u \tag{1}$$

$$\frac{\partial v}{\partial t}+u\frac{\partial v}{\partial x}+v\frac{\partial v}{\partial y}+\frac{\partial p}{\partial y}=\frac{1}{R}\nabla^2 v \tag{2}$$

$$\frac{\partial u}{\partial x}+\frac{\partial u}{\partial y}=0 \tag{3}$$

Here, x and u are the coordinate and velocity in the streamwise direction, y and v are the coordinate and velocity in the direction normal to the boundary, p is the fluid pressure divided by the mass density, and $R=U_\infty\delta/\nu$ is the Reynolds number, where ν is the kinematic viscosity. The Laplacian operator is

$$\nabla^2=\frac{\partial^2}{\partial x^2}+\frac{\partial^2}{\partial y^2}$$

It is convenient to define a base flow, denoted by capital letters, which satisfies the steady flow equations:

$$U\frac{\partial U}{\partial x}+V\frac{\partial U}{\partial y}+\frac{\partial P}{\partial x}=\frac{1}{R}\nabla^2 U \tag{4}$$

$$U\frac{\partial V}{\partial x}+V\frac{\partial V}{\partial y}+\frac{\partial P}{\partial y}=\frac{1}{R}\nabla^2 V \tag{5}$$

$$\frac{\partial U}{\partial x}+\frac{\partial V}{\partial y}=0 \tag{6}$$

For high Reynolds number flows about solid boundaries where thin boundary layers form, these equations can be solved by using boundary-layer/potential flow techniques. Disturbances to the base flow then satisfy

$$\frac{\partial u'}{\partial t}+U\frac{\partial u'}{\partial x}+u'\frac{\partial U}{\partial x}+u'\frac{\partial u'}{\partial x}+V\frac{\partial u'}{\partial y}+v'\frac{\partial U}{\partial y}+v'\frac{\partial u'}{\partial y}+\frac{\partial p'}{\partial x}=\frac{1}{R}\nabla^2 u' \tag{7}$$

$$\frac{\partial v'}{\partial t}+U\frac{\partial v'}{\partial x}+u'\frac{\partial V}{\partial x}+u'\frac{\partial v'}{\partial x}+V\frac{\partial v'}{\partial y}+v'\frac{\partial V}{\partial y}+v'\frac{\partial v'}{\partial y}+\frac{\partial p'}{\partial y}=\frac{1}{R}\nabla^2 v' \tag{8}$$

$$\frac{\partial u'}{\partial x}+\frac{\partial v'}{\partial y}=0 \tag{9}$$

The boundary conditions appropriate to these equations are that the disturbance quantities vanish far from the solid boundary,

$$u',v',p'\to 0 \text{ as } y\to\infty \tag{10}$$

that the disturbance velocities vanish on the solid boundary,

$$u'=v'=0 \text{ at } y=0 \tag{11}$$

and, by evaluating Eq. (8) on the boundary and using Eq. (9), that

$$\frac{\partial p'}{\partial y}=-\frac{1}{R}\frac{\partial^2 u'}{\partial x\partial y} \text{ at } y=0 \tag{12}$$

Boundary conditions in the streamwise direction depend on the nature of the problem being solved.

The technique developed in this work, with a proper formulation of boundary conditions, are capable of solving the disturbance equations for the most general base flows, but here we shall consider the special case of parallel flow, when $U=U(y)$ and $V=0$. Strictly speaking, the only such flow satisfying this condition is the parabolic distribution. In the thin boundary layers that form at high Reynolds numbers, however, the normal velocity field is extremely small, and the assumption of parallel flow is nearly met (Ref. 3, pp. 116 ff). This is not to say, of course, that nonparallel effects may not be important, but, for the purposes of making a quantitative evaluation of the numerical approach, it seems appropriate to consider parallel flows for which analytical solutions are readily available. The disturbance equations then can be simplified to the form

$$\frac{\partial u'}{\partial t}+U\frac{\partial u'}{\partial x}+u'\frac{\partial u'}{\partial x}+v'\frac{dU}{dy}+v'\frac{\partial u'}{\partial y}+\frac{\partial p'}{\partial x}=\frac{1}{R}\nabla^2 u' \tag{13}$$

$$\frac{\partial v'}{\partial t}+U\frac{\partial v'}{\partial x}+u'\frac{\partial v'}{\partial x}+v'\frac{\partial v'}{\partial y}+\frac{\partial p'}{\partial y}=\frac{1}{R}\nabla^2 v' \tag{14}$$

$$\frac{\partial u'}{\partial x}+\frac{\partial v'}{\partial y}=0 \tag{15}$$

The linearized forms of Eqs. (13-15) have been studied extensively, especially the growth rates and spectral properties of periodic disturbances. The assumptions of linearization and periodicity allow the preceding equations to be transformed into a single ordinary differential equation, the Orr-Sommerfeld equation. The resulting body of knowledge, known as linear stability theory (LST), offers a quantitative test of the direct numerical solution of the equations.

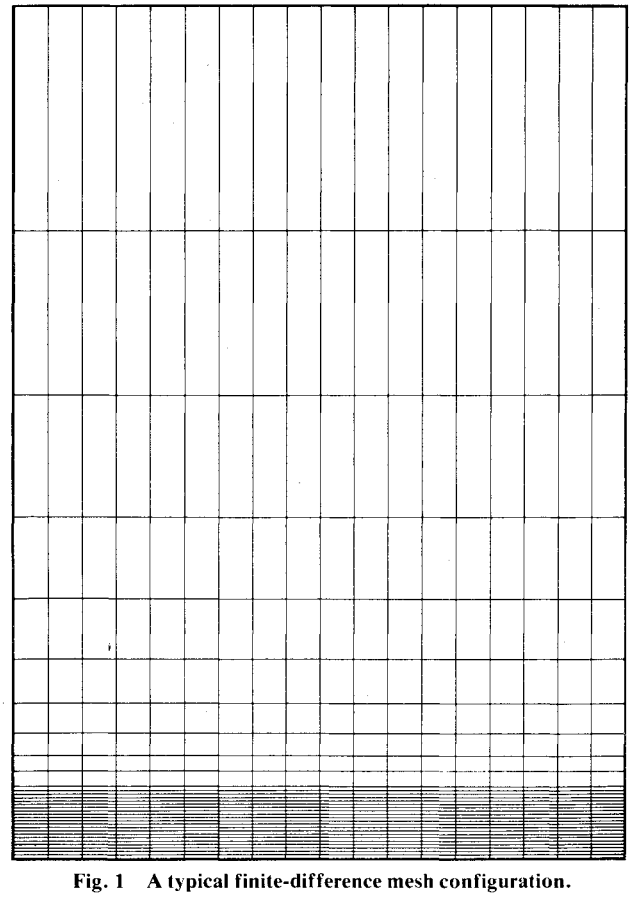

Fig. 1 A typical finite-difference mesh configuration.

The results discussed in this work are for parallel flows in which U is taken as the horizontal component of the velocity over a flat plate, the Blasius profile. In order to compare with LST, the disturbance flow is assumed to be periodic with wavelength λ in the streamwise direction. There are then two parameters describing small-amplitude motion, the Reynolds number R, and the dimensionless wave number $\alpha = 2\pi\delta/\lambda$.

III. Numerical Solution Technique

Equations (13-15) subject to boundary conditions (10-12) are to be solved in a region $0 \le x \le \lambda/\delta$ and $0 \le y < \infty$. The region first is divided into finite-sized cells, of constant size in the horizontal and variably spaced in the vertical (see Fig. 1). Within each cell, the horizontal velocity is defined at the center of the left face, the vertical velocity at the center of the bottom face, and the pressure at the cell center (see Fig. 2), in the usual staggered mesh configuration.

The following finite-difference form was used to represent the time rate of change of the discrete velocities:

$$\left(\frac{\partial u}{\partial t}\right)_{i,j} = -\frac{1}{2\delta x} U_j (u_{i+1,j} - u_{i-1,j})$$
$$- \frac{1}{4\delta x}\left[u_{i+1,j}(u_{i+1,j}+u_{i,j}) - u_{i-1,j}(u_{i,j}+u_{i-1,j})\right]$$
$$- \frac{1}{4\delta y_j}\left[u_{i,j+1}(v_{i,j+1}+v_{i-1,j+1}) - u_{i,j-1}(v_{i,j}+v_{i-1,j})\right]$$
$$- \frac{1}{4}\left(\frac{dU}{dy}\right)_j (v_{i,j}+v_{i,j+1}+v_{i-1,j}+v_{i-1,j+1})$$
$$- \frac{1}{\delta x}(p_{i,j}-p_{i-1,j}) + \frac{1}{R(\delta x)^2}(u_{i+1,j}-2u_{i,j}+u_{i-1,j})$$
$$+ \frac{1}{R\delta y_j}\left[\frac{1}{\delta y_{j+1/2}}(u_{i,j+1}-u_{i,j}) - \frac{1}{\delta y_{j-1/2}}(u_{i,j}-u_{i,j-1})\right] \quad (16)$$

$$\left(\frac{\partial v}{\partial t}\right)_{i,j} = -\frac{1}{4\delta x}(U_j + U_{j-1})(v_{i+1,j} - v_{i-1,j})$$
$$- \frac{1}{4\delta x}\left[v_{i+1,j}(u_{i+1,j}+u_{i+1,j-1}) - v_{i-1,j}(u_{i,j}+u_{i,j-1})\right]$$
$$- \frac{1}{4\delta y_{j-1/2}}\left[v_{i,j+1}(v_{i,j}+v_{i,j+1}) - v_{i,j-1}(v_{i,j}+v_{i,j-1})\right]$$
$$- \frac{1}{\delta y_{j-1/2}}(p_{i,j}-p_{i,j-1}) + \frac{1}{R(\delta x)^2}(v_{i+1,j}-2v_{i,j}+v_{i-1,j})$$
$$+ \frac{1}{R\delta y_{j-1/2}}\left[\frac{1}{\delta y_j}(v_{i,j+1}-v_{i,j}) - \frac{1}{\delta y_{j-1}}(v_{i,j}-v_{i,j-1})\right] \quad (17)$$

Here $\delta y_{j-1/2} = \frac{1}{2}(\delta y_j + \delta y_{j-1})$. Also, we have dropped the prime from the lower-case quantities since no confusion with total velocities or pressures can result. The difference form used for the nonlinear terms is that of Piacsek and Williams.[4]

If I and J represent the total number of columns and rows used, with columns $i=1$ and I and rows $j=1$ and J being boundary cells outside the physical domain, then the boundary conditions given by Eqs. (10-12) become

$$v_{i,J} = 0, \quad u_{i,J} = -u_{i,J-1}, \quad p_{i,J} = -p_{i,J-1} \quad (18)$$

$$v_{i,2} = 0, \quad u_{i,1} = -u_{i,2}, \quad p_{i,1} = p_{i,2} + \frac{2}{R\delta x}(u_{i+1,2} - u_{i,2}) \quad (19)$$

$$u_{1,j} = u_{2,j}, \quad v_{1,j} = v_{2,j}, \quad p_{1,j} = p_{2,j} \quad (20)$$

$$u_{I,j} = u_{I-1,j}, \quad v_{I,j} = v_{I-1,j}, \quad p_{I,j} = p_{I-1,j} \quad (21)$$

The pressure field is determined so as to guarantee that Eq. (15) is satisfied. Before discussing the details of how the pressure is calculated, it is convenient to define the bracketed finite-difference operators through the equations

$$\left(\frac{\partial u}{\partial t}\right)_{i,j} = \left[\frac{\partial u}{\partial t}\right]_{i,j} - \frac{1}{\delta x}(p_{i,j} - p_{i-1,j}) \quad (22)$$

$$\left(\frac{\partial v}{\partial t}\right)_{i,j} = \left[\frac{\partial v}{\partial t}\right]_{i,j} - \frac{1}{\delta y_{j-1/2}}(p_{i,j} - p_{i,j-1}) \quad (23)$$

That is, they are the time rate-of-change operators without the pressure terms. The solutions are advanced in time by the time-average, implicit algorithm

$$\phi_{i,j}^{n+1} = \phi_{i,j}^{n} + \frac{1}{2}\delta t\left[\left(\frac{\partial \phi}{\partial t}\right)_{i,j}^{n} + \left(\frac{\partial \phi}{\partial t}\right)_{i,j}^{n+1}\right] \quad (24)$$

where the superscript indicates the time level and δt is the finite time step. This scheme, when used with central space differencing, is second-order accurate in space and time and introduces no numerical dissipation (Ref. 5, p. 84); this is of crucial importance to the calculation of a flow where the effect of a very small, real viscosity is the principal issue. The use of the Piascek and Williams differencing algorithm insures energy conservation for variable velocity and mesh. The velocity fields then are given by the formulas

$$u_{i,j}^{n+1} = u_{i,j}^{n} + \frac{1}{2}\delta t\left[\left(\frac{\partial u}{\partial t}\right)_{i,j}^{n} + \left[\frac{\partial u}{\partial t}\right]_{i,j}\right] - \frac{\delta t}{2\delta x}(p_{i,j}^{n+1} - p_{i-1,j}^{n+1}) \quad (25)$$

$$u_{i,j}^{n+1} \equiv \tilde{u}_{i,j} - \frac{\delta t}{2\delta x}(p_{i,j}^{n+1} - p_{i-1,j}^{n+1}) \quad (26)$$

and

$$v_{i,j}^{n+1} = v_{i,j}^{n} + \frac{1}{2}\delta t\left[\left(\frac{\partial v}{\partial t}\right)_{i,j}^{n} + \left[\frac{\partial v}{\partial t}\right]_{i,j}\right]$$
$$- \frac{\delta t}{2\delta y_{j-1/2}}(p_{i,j}^{n+1} - p_{i,j-1}^{n+1}) \quad (27)$$

$$v_{i,j}^{n+1} \equiv \tilde{v}_{i,j} - \frac{\delta t}{2\delta y_{j-1/2}}(p_{i,j}^{n+1} - p_{i,j-1}^{n+1}) \quad (28)$$

Because the time derivatives involve products of the fluid velocities, Eqs. (26) and (28) are coupled, nonlinear algebraic equations. Furthermore, the pressure field at the new time level must be chosen so that the new velocities are divergence-

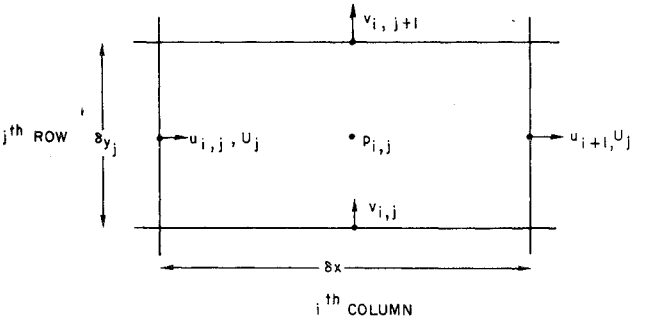

Fig. 2 Variable placement within a finite-difference cell.

free; that is,

$$\frac{1}{\delta x}(u_{i+1,j}^{n+1}-u_{i,j}^{n+1})+\frac{1}{\delta y_j}(v_{i,j+1}^{n+1}-v_{i,j}^{n+1})=0 \qquad (29)$$

This last relation, when expressions (26) and (29) are used to eliminate the v^{n+1} and u^{n+1}, leads to the following linear, elliptic boundary-value problem for the pressures:

$$\frac{1}{(\delta x)^2}\left[p_{i+1,j}^{n+1}-2p_{i,j}^{n+1}+p_{i-1,j}^{n+1}\right]+\frac{1}{\delta y_j}\times\left[\frac{1}{\delta y_{j+\frac{1}{2}}}(p_{i,j+1}^{n+1}-p_{i,j}^{n+1})-\frac{1}{\delta y_{j-\frac{1}{2}}}(p_{i,j}^{n+1}-p_{i,j-1}^{n+1})\right]=\frac{2}{\delta t}\left[\frac{1}{\delta x}(\tilde{u}_{i+1,j}-\tilde{u}_{i,j})+\frac{1}{\delta y_j}(\tilde{v}_{i,j+1}-\tilde{v}_{i,j})\right] \qquad (30)$$

The solution is advanced to the $n+1$ time step through the following iterative scheme:

1) The new velocities and pressures are set equal to the previous values.

2) The tilda velocities are computed using Eqs. (25-28).

3) The system of Eq. (30) is inverted to obtain a better guess of the pressure.

4) Equations (26) and (28) are used to obtain a better guess of the velocities.

5) Steps 2-4 are repeated until the quantities do not change by some predetermined amount.

The solution of Eq. (30) is obtained by decomposing and backsolving the banded pressure matrix using the Cholesky method. The manipulations are carried out by an especially efficient routine developed by M. Vander Vorst of JAYCOR.

Stability and accuracy considerations require that the time step does not exceed values imposed by the advection and diffusion terms:

$$\delta t<\min\left\{\frac{\delta x}{|U_j+u_{i,j}|},\ \frac{\delta y_j}{|v_{i,j}|},\ \frac{R}{4}(\delta x)^2,\ \frac{R}{4}(\delta y_j)^2\right\} \qquad (31)$$

Experience has shown that, if δt is taken to be one-quarter of the maximum time step allowed, then at least three significant figures are obtained in the velocity and pressure fields with five iterations.

IV. Comparison with Linear Stability Theory

The linearized forms of Eqs. (13-15) have been studied in detail, e.g., by Wazzan et al.[6] and Jordinson,[7] the case of greatest interest being when U takes on the Blasius profile (see also the reviews by Tani[8] and Reshotko[9]). Not only have detailed quantitative solutions been obtained, but the predicted fluid-dynamic behavior is in close agreement with experimental observation of small disturbances in the boundary layer of a flat plate (for example, see Ross et al.[10]). Comparison with LST offers, then, a meaningful test of the numerical approach.

When the disturbances are periodic in space, the eigenfunctions are characterized by the two parameters α and R. Figure 3 shows the curve of neutral stability, that is, those disturbances that neither grow nor die out, as determined by Jordinson; points inside the curve are unstable flows, and those outside are stable. Jordinson's calculations were for temporally periodic disturbances, but, for points near the neutral stability curve, the solutions are the same as for spatially periodic disturbances. Below the critical Reynolds number of 520, LST predicts that all disturbances die out, and thus that the boundary layer is completely stable.

To compare with the predictions of LST, a series of numerical experiments was conducted using the full, nonlinear equation set discussed in the last section but using

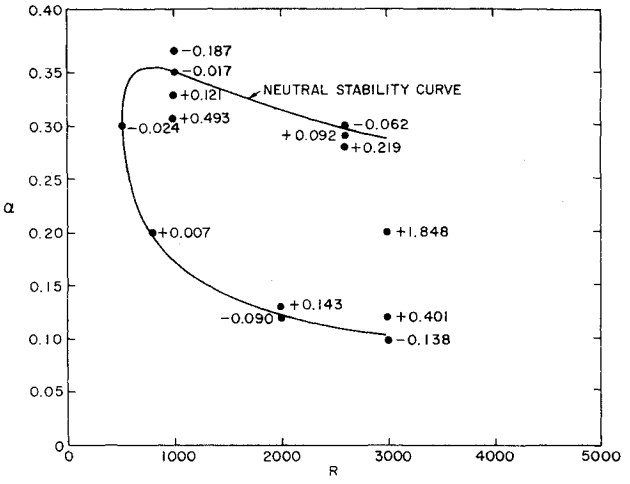

Fig. 3 Neutral stability curve and cases for which numerical calculations have been made. Numbers indicate the logarithmic energy change per period.

disturbances at small amplitude. In each case, the mesh consisted of 18 constant-sized cells in the horizontal direction, spanning one spatial period, and 34 variably sized cells in the vertical. The smallest vertical cells were 0.1δ wide, whereas above $y=2.0$ the cells expanded geometrically so that the top of the last cell was almost 100δ from the solid boundary. Recall that y is the vertical coordinate in multiples at δ. Figure 1 shows the mesh configuration up to $y=25$. The top boundary appears not to influence the results, since placing it further away led to no change in the flow properties. The base flow was given a small disturbance, whose maximum horizontal velocity was 0.0001 U_∞, and which was then allowed to evolve toward a final state.

The circles shown in Fig. 3 represent the matrix of numerical experiments conducted. The numbers indicate the logarithmic energy change per period of oscillation:

$$\theta=\ell_n\frac{E(t+T)}{E(t)}, \quad T=\text{period of disturbance} \qquad (32)$$

where the energy is defined by

$$E=\iint dx\,dy\,\tfrac{1}{2}(u'^2+v'^2)$$

This quantity has not yet reached a final value in all cases, so the quoted value, taken at the end of a run, may change slightly. Figure 4 shows the variation with time of the energy for most of the runs.

Figure 5 compares the time variation of production and dissipation for one case near the neutral curve, where

$$\text{production}=\iint dx\,dy\left(-u'v'\frac{dU}{dy}\right) \qquad (33)$$

$$\text{dissipation}=-\iint dx\,dy(u'\nabla^2u'+v'\nabla^2v') \qquad (34)$$

The production is the rate at which energy is extracted from the base flow, while dissipation is the rate at which it is lost to heat. The rates should be equal for a neutral case. Since the initial disturbance is not a pure eigenmode of the system, and since neighboring modes die out slowly, the flow requires a considerable time to settle into a single, pure motion. That difference distinguishes a true initial-value problem from the eigenvalue problem posed by LST.

Since negative values in Fig. 3 indicate damped motion and positive values indicate growth, the results are not in conflict with LST. In fact, when nearby pairs of numerical calculations, one showing growth and the other decay, are

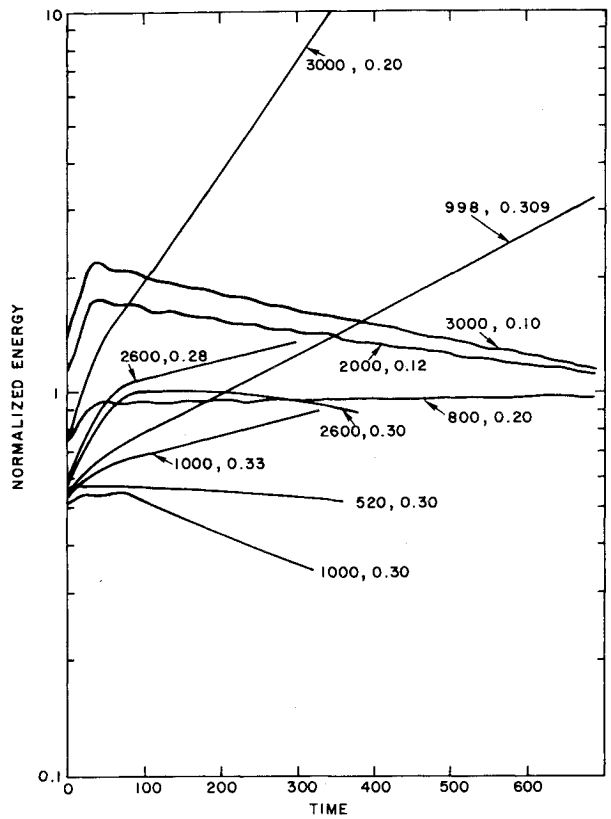

Fig. 4 Time variation of the flow energy for several numerical calculations.

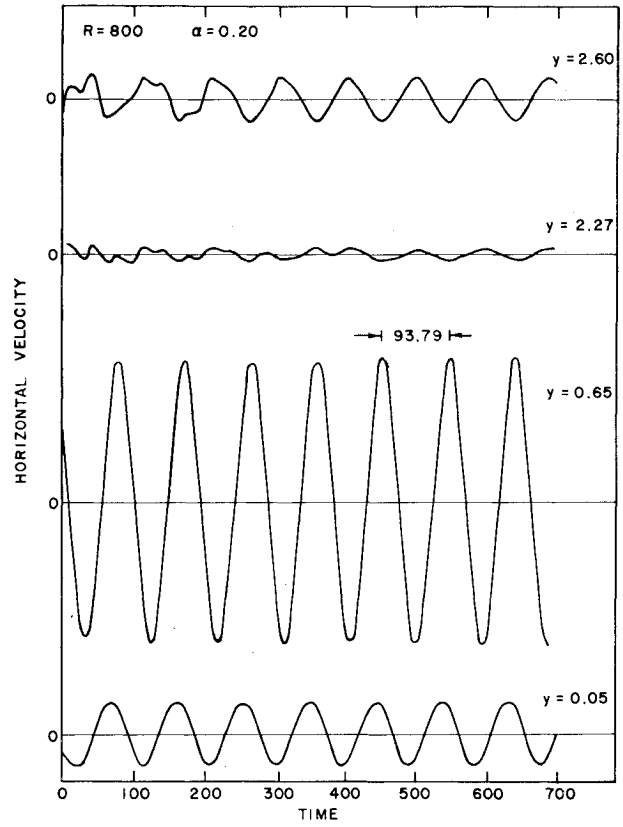

Fig. 6 Time traces of the horizontal velocity component for various distances from the wall.

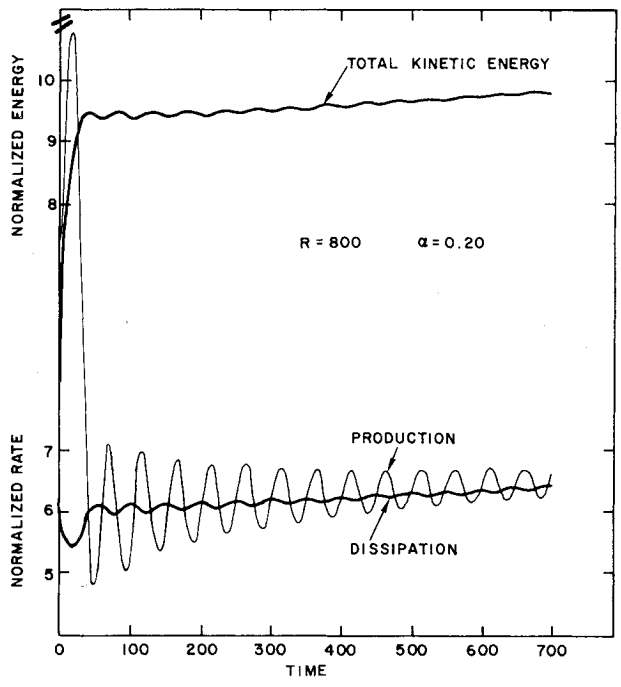

Fig. 5 Comparison of production and dissipation rates during the relaxation to a final state for a case near the neutral curve.

used to interpolate a neutral condition, the results agree with LST to within a few percent for both the wave number and frequency (see Table 1). Here, β is the dimensionless frequency of oscillation. The numerical calculation appears to have reproduced the overall energy balance and time behavior in the flow correctly.

Next, details of the flowfield were examined. Figure 6 shows the variation with time of the horizontal disturbance velocity at a particular streamwise position and for various distances from the wall. This format is analogous to the continuous output of a velocity probe and shows the experimentally observed pattern (Ref. 3, p. 403) that the amplitude grows with distance from the wall, reaches a peak, suffers a phase reversal, and dies out. The calculated period of oscillation is 93.79, while Jordinson's calculated value is 93.48.

Figures 7 and 8 compare the amplitude and phase variation with distance from the wall found from a numerical calculation and Jordinson's eigenfunction solution. The comparison shows that the details of the flow are reproduced completely, including the subtle phase variations occurring in the flow near the wall. The numerical calculation appears to have reproduced the flow details correctly, as well as the overall energy balances.

Table 1 Results of numerical calculations

R		α	β
1000	Numerical	0.348	0.128
	LST	0.351	0.131
2000	Numerical	0.1239	0.0327
	LST	0.1234	0.0332
2600	Numerical	0.295	0.0927
	LST	0.297	0.0947
3000	Numerical	0.1051	0.0257
	LST	0.1029	0.0235
α		R	β
0.30	Numerical	530	0.1167
	LST	521	0.1175

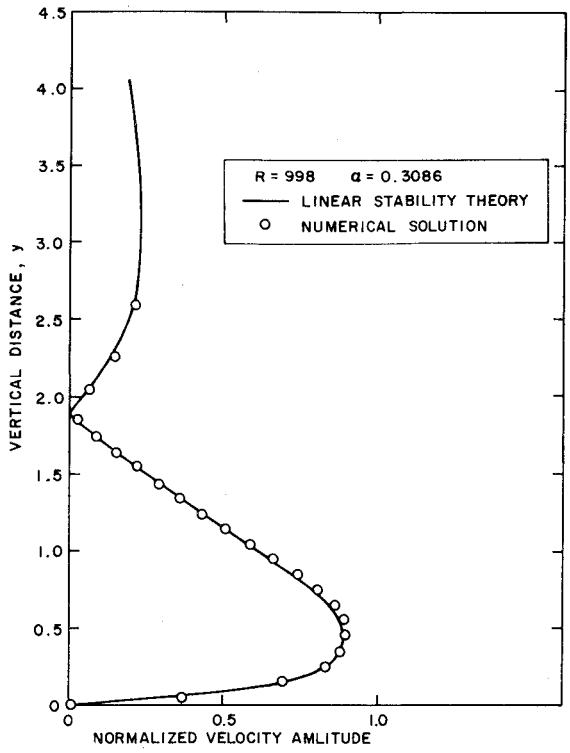

Fig. 7 Comparison of horizontal velocity amplitude variation.

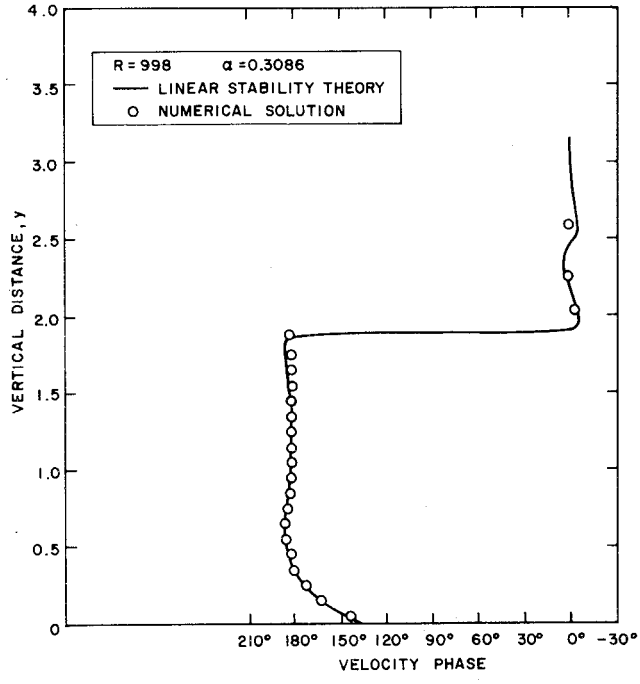

Fig. 8 Comparison of horizontal velocity phase variation.

V. Finite-Amplitude Effects

The previous comparisons with linear stability theory suggest that the behavior of small-amplitude disturbances is being correctly computed numerically. A series of calculations then was performed to determine the effects of finite amplitude. In each case, the initial disturbance had the same spatial distribution, but the maximum amplitude of u' was taken as 0.0001, 0.01, 0.03, and 0.1 of U_∞. The results show a trend conjectured by nonlinear stability theories[11] that finite-amplitude effects can be destabilizing. It must be borne in mind, however, that the ability to numerically calculate nonlinear fluid-dynamics processes of this type has yet to be

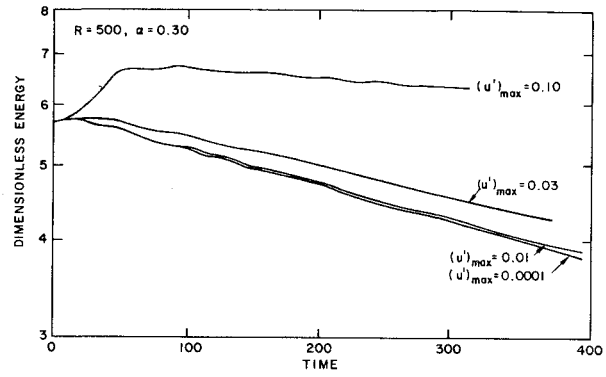

Fig. 9 Variation of energy with time for various amplitudes of the initial disturbance.

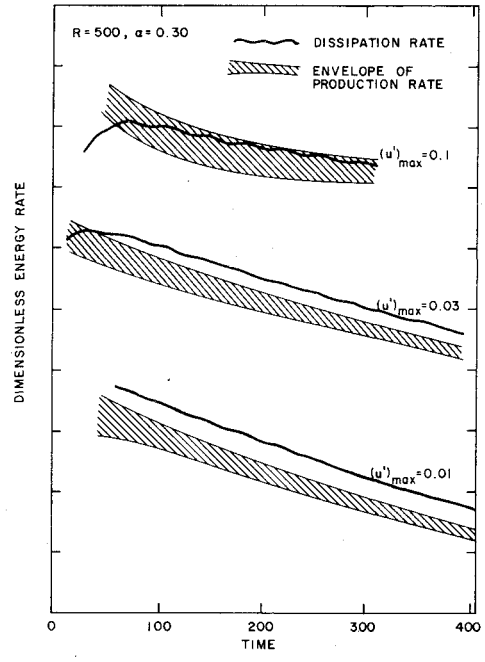

Fig. 10 Variation of production and dissipation rates for various initial disturbance amplitudes.

established firmly, so that these results should be treated as demonstrating the potential of the method rather than rigorous mathematical results. Figure 9 shows the variation of the total energy in the disturbance flow in each case, normalized to the same initial value. The case considered is $R = 500$, $\alpha = 0.30$, a point in the subcritical regime where LST predicts all disturbances to die out. At the smallest amplitudes, the disturbance dies out at a rate consistent with LST. For $(u')_{max} = 0.03$, however, the decay has been decreased noticeably whereas for $(u')_{max} = 0.1$ the disturbance is almost neutrally stable. Although a truly unstable state was not achieved, the destabilizing effects seem to be definite. A similar variation is seen for unstable small-amplitude modes: as they grow to finite amplitude, the rate of growth increases.

Figure 10 further illustrates the effects of finite amplitude, by considering the integrated production and dissipation rates for the case $R = 500$, $\alpha = 0.30$. At small amplitudes, dissipation always exceeds production, and the disturbance monotonically dies out. At $(u')_{max} = 0.1$, however, the production exceeds dissipation during part of the oscillation, so that for some time it grows and for some time it is damped. The damped periods are greater, so that the disturbance is dying out overall, but a balance is almost being struck.

The accuracy of finite-difference techniques for large-amplitude phenomena is difficult to assess, and so a detailed

investigation probably is not warranted at this time. For example, the spatial resolution of very high order harmonics generated by the nonlinear interactions is limited and eventually would necessitate calculations at greater resolution. In the light of the other uncertainties of finite-difference representation of large-amplitude effects, spatial resolution studies were not conducted. Still, the results indicate that the numerical solution technique used in this work may be a useful tool in studying finite-amplitude effects in the boundary layer.

VI. Concluding Remarks

The finite-difference method presented here has been shown to reproduce accurately analytical results concerning boundary-layer stability with a modest storage requirement (612 interior cells) and modest computational time (typically 2-5 min of CDC 7600 central processor time). This efficiency, coupled with encouraging results in the nonlinear regime, makes the approach an attractive candidate for studying the large-amplitude, three-dimensional motion that accompanies boundary-layer transition.

Acknowledgments

This research was sponsored by the Space and Missile Systems Organization and the Air Force Office of Scientific Research (AFSC), U.S. Air Force, under Contract No. F49620-77-C-0030. The U.S. Government is authorized to reproduce and distribute reprints for governmental purposes notwithstanding any copyright notation hereon.

References

[1] Fasel, H., "Investigation of the Stability of Boundary Layers by a Finite-Difference Model of the Navier-Stokes Equations," *Journal of Fluid Mechanics*, Vol. 78, Pt. 2, 1976, p. 355.

[2] Murdock, J. W., "A Numerical Study of Nonlinear Effects on Boundary-Layer Stability," *AIAA Journal*, Vol. 15, Aug. 1977, pp. 1167-1173.

[3] Schlichting, H., *Boundary Layer Theory*, 4th ed., McGraw-Hill, New York, 1960.

[4] Piacsek, S. A. and Williams, G. P., "Conservation Properties of Convection Differencing Schemes," *Journal of Computational Physics*, Vol. 6, 1970, p. 392.

[5] Roache, P. J., *Computational Fluid Dynamics*, Hermosa Publishers, Albuquerque, N. Mex., 1976.

[6] Wazzan, A. R., Okamura, T. T., and Smith, A. M. O., "Spatial and Temporal Stability Charts for the Falkner-Skan Boundary-Layer Profiles," McDonald-Douglas Co., Rept. DAC-67086, 1968.

[7] Jordinson, R., "The Flat Plate Boundary Layer. Part 1. Numerical Integration of the Orr-Sommerfeld Equation," *Journal of Fluid Mechanics*, Vol. 43, Pt. 4, 1970, p. 801.

[8] Tani, I. T., "Boundary-Layer Transition," *Annual Reviews of Fluid Mechanics*, Vol. 1, 1969, p. 169.

[9] Reshtko, E.,"Boundary Layer Stability and Transition," *Annual Reviews of Fluid Mechanics*, Vol. 8, 1976, p. 311.

[10] Ross, J. A., Barnes, F. H., Burns, J. G., and Ross, M. A. S., "The Flat Plate Boundary Layer. Part 3. Comparison of Theory with Experiment," *Journal of Fluid Mechanics*, Vol. 43, Pt. 2, 1970, p. 819.

[11] Stewartson, K., "Some Aspects of Nonlinear Stability Theory," *Polish Academy of Sciences*, Vol. 7, 1975, p. 101.